VINEYARD CLASSIFICATION USING MACHINE LEARNING TECHNIQUES APPLIED TO RGB-UAV IMAGERY

Luís Pádua[(1,2)], Telmo Adão[(1,2)], Jonáš Hruška[(1)], Nathalie Guimarães[(1)], Pedro Marques[(1,3)], Emanuel Peres[(1,2)] and Joaquim J. Sousa[(1,2)]

[1]University of Trás-os-Montes e Alto Douro, Vila Real, Portugal
[2]Centre for Robotics in Industry and Intelligent Systems, INESC-TEC, Porto, Portugal
[3]Centre for the Research and Technology of Agro-Environmental and Biological Sciences, Vila Real, Portugal

ABSTRACT

In this study machine learning methods were applied to RGB data obtained by an unmanned aerial vehicle (UAV) to assess this effectiveness in vineyard classification. The very high-resolution UAV-based imagery was subjected to a photogrammetric processing allowing the generation of different outcomes: orthophoto mosaic, crop surface model and five vegetation indices. The orthophoto mosaic was used in an object-based image analysis approach to group pixels with similar values into objects. Three machine learning techniques—support vector machine (SVM), random forest (RF) and artificial neural network (ANN)—were applied to classify the data into four classes: grapevine, shadow, soil and other vegetation. The data were divided with 22% (n=240, 60 per class) for training purposes and 78% (n = 850) for testing purposes. The mean value of the objects from each feature were used to create a dataset for prediction. The results demonstrated that both RF and ANN models showed a good performance, yet the RF classifier achieved better results.

Index Terms— Precision viticulture, object-based image analysis, artificial neural networks, random forests, support vector machines

1. INTRODUCTION

Grapevine segmentation and classification of different features in a vineyard represents a key-task for optimal management of the parcel. The use of high-resolution imagery acquired from unmanned aerial vehicles (UAVs) provide different approaches to achieve this goal. The most commonly used methods are based on the use of image segmentation techniques [1], or by filtering the grapevine height [2], [3]. More recently, unsupervised or supervised machine learning techniques [4] are taking more prominence. However, most of the studies in the literature refers to very well managed commercial vineyards with good contrast between the vineyard and the ground, in which, very few or no missing plants are presented [4]. Moreover, studies that use very-high resolution imagery for similar purposes, generally rely in the usage of more expensive sensors for data acquisition [1], [5], as multispectral imagery.

In this study, a cost-effective light-weight UAV was used to acquire RGB imagery aiming the classification of grapevine vegetation and other features usually presented within a vineyard plot. Three machine learning approaches were assessed: support vector machines (SVM), artificial neural networks (ANN), and random forests (RF). Furthermore, an object-based image analysis (OBIA) approach was used to predict the distribution of the different classes on the different machine learning techniques used in this study.

2. MATERIAL AND METHODS

2.1. Study area description

The vineyard plot used in this study (Fig. 1) is located in the geographical area of the Douro Demarcated Region, within the campus of the University of Trás-os-Montes e Alto Douro (Vila Real, Portugal). The grapevine plants (cv. *Malvasia Fina*) are 1.20 m apart and the space between its 22 rows is 1.80 m. This vineyard plot is affected by grapevine trunk diseases which caused a high number of missing grapevine plants along the vine rows.

Fig. 1. Overview of the studied vineyard plot.

2.2. Data acquisition and photogrammetric processing

A multi-rotor DJI Phantom 4 UAV (DJI, Shenzhen, China), equipped with an RGB sensor (12.4 MP) was used to acquire the aerial imagery. The flight mission consisted in a crosshatch pattern at 40 m flight height, being the front and side overlap of 80% and 70%, respectively. The flight was performed on 24 July 2019, close to solar noon and under clear skies. The flight mission took approximately five minutes and a total of 88 images were acquired, covering an area of approximately 2 ha with a spatial resolution of less than 2 cm (0.0185 m).

The photogrammetric processing of the acquired UAV-based RGB imagery was conducted using the Pix4Dmapper Pro (Pix4D SA, Lausanne, Switzerland). The dense point cloud was computed with a high point density (total of 21 million points, with an average density of 1771 points per m³). As outcomes, an orthophoto mosaic,

a Digital Surface Model (DSM) and a Digital Terrain Model (DTM) were generated.

The orthophoto mosaic was clipped to the region of interest using QGIS software. Then, several vegetation indices were computed, as presented in TABLE I. The DSM and the DTM were used to compute a Crop Surface Model (CSM), by subtracting the altitude values of the DTM to the DSM.

TABLE I. VEGETATION INDICES USED IN THIS STUDY.

Vegetation index	Equation	Reference
Green-Red Vegetation Index	$GRVI = \dfrac{G - R}{G + R}$	[6]
Green-Blue Vegetation Index	$GBVI = \dfrac{G - B}{G + B}$	[7]
Red Green Blue Vegetation Index	$RGBVI = \dfrac{G^2 - R \times B}{G^2 + R \times B}$	[8]
Excess Green	$ExG = 2g - r - b$	[9]
Visible Atmospherically Resistant Index	$VARI = \dfrac{G - R}{G + R - B}$	[10]

where $r = \frac{R}{R+G+B}$, $g = \frac{G}{R+G+B}$, and $b = \frac{B}{R+G+B}$; R, G and B are the pixel values of the Red, Green and Blue bands, respectively.

2.3. Object-based image analysis

The object-based image analysis was performed in QGIS using the Orfeo ToolBox (OTB) [11]. For this purpose, large-scale segmentation using the mean shift [12] was applied through the use of the "LargeScaleMeanShift" function. By providing as input a raster image of the study area, a vector data file was generated using the MeanShift algorithm. In this study, the orthophoto mosaic was used as input and the spatial and range radius were set to, 12 and 18, respectively. Moreover, the minimum segment size was defined to 200, thus ensuring that regions smaller than this parameter are merged into similar neighbouring regions.

2.4. Vineyard classification

The following classes were defined, according to the characteristics of the surveyed vineyard: (1) soil—areas without vegetation, mainly composed by bare soil, small rocks and dry vegetation; (2) shadow—casted by grapevines, vineyard posts and trees in the surroundings of the vineyard plot; (3) other vegetation—composed by other type of vegetation than grapevines, as inter-row vegetation and weeds; and (4) grapevine—composed by the vegetation belonging to grapevines.

For classification purposes, three machine learning algorithms were used: SVM, RF, and ANN. Since the evaluated methods are supervised, a set of training and testing samples are required. Therefore, a set of 400 squares with 20×20 cm area were spread throughout the study area, evenly distributed through the four defined classes, representing a total of 100 samples per class. The number and size of the squares was selected to both cover the majority of different cases and to minimise the inclusion of multiple classes in a single square. From the 400 sample squares, 240 were used for training. The trained models were then tested using the remaining 160 squares. Apart from the 160 squares, three transects were also considered for testing the classifiers (location in Fig. 1.), being one in a vine row (68 m), and two between rows (42 m and 27 m). The transects were divided and buffered to create 20×20 cm square samples (total of 690) and were classified according to one

of the analysed classes. The models obtained from each classifier were used to predict upon the objects created using the mean shift algorithm.

Following the creation and division of the samples, different features were estimated for the objects and squares, which rely on the mean values of the vegetation indices presented in TABLE I. Along with the vegetation indices, the mean value of the red, green and blue bands, their normalized values (r, g and b) and the height values from CSM were also used.

For training and validation purposes, the "TrainVectorClassifier" function and the "VectorClassifier" function of the OTB toolbox were used. The SVM model, based in the LIBSVM [13], used a linear kernel, being the penalty set using the cost parameters C with a value of one. The used ANN and RF classifiers are both based in the OpenCV machine learning library. The RF model values were configured as following: five of maximum tree depth, 10 as minimum number of samples in each note, 100 as maximum number of trees in the forest and an out-of-bag (OOB) error of 0.01. Regarding the ANN, it was trained with a resilient back-propagation algorithm with four neurons in each intermediate layer, a symmetrical sigmoid function for neuron activation with alpha and beta parameters set to one and a maximum number of 1000 of iterations.

2.5. Accuracy verification

To evaluate the classification of the models obtained from the machine learning classifiers the resultant confusion matrices were analysed. To provide a general perspective of the model behaviour, the f1-score, kappa coefficient and the overall accuracy were computed. While the overall accuracy indicates the proportion of correct classifications in the total number of samples, the kappa coefficient evaluates the performed classification, considering the possibility of the agreement occurring by chance. Moreover, the area estimated for each class was also evaluated.

3. EXPERIMENTAL RESULTS

3.1. Data characterization

A data analysis was performed to assess the behaviour of each class of the features used in this study. Fig. 2 presents the mean values of each feature, per class, where the soil class presents highest overall values in the RGB bands (Fig. 2a). On the contrary, the shadow class presents the lowest values. The remaining classes show similar values for green band, but the grapevine class presents lower values for red and blue bands, when compared to other vegetation class. When analysing band's normalized values (Fig. 2b), the normalized green band stands out in the grapevine vegetation, being that the same tendency verified for the vegetation indices (Fig. 2c). Moreover, the grapevine class present higher mean values than the remaining classes, followed by the other vegetation. These values can be explained by the greener colour from its leaves. Contrary to the grapevine class, the shadow class present lower mean values than the other classes, where, this can be related to its darker characteristics. Regarding the soil class, it present negative values for GRVI and VARI. Concerning the mean height values extracted from the CSM (Fig. 2d), values above zero were only observed in shadow and grapevine classes, where, height values present in shadow can be related to the presence of shadows in the grapevine canopy.
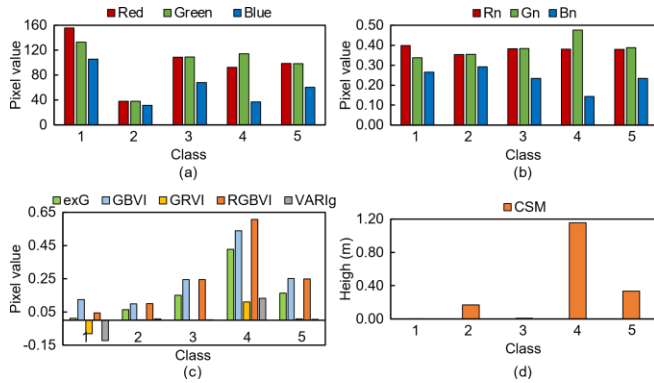
Fig. 2. Mean values, per class, of each feature: (a) bands of the orthophoto mosaic; (b) normalized bands; (c) vegetation indices; and (d) crop surface model (CSM). Values obtained from the 240 sample squares, used for training. 1: soil; 2: shadow; 3: other vegeation; 4: grapevine; 5: overall mean values.

3.2. Vineyard classification accuracy

Regarding the overall accuracy, the results of the testing phase of the three tested classifiers (SVM, RF and ANN) showed different performances (Table II). The higher overall accuracy was achieved by RF classifier (88%), followed by ANN (86%) and SVM with the lowest performance (45%). Both ANN and RF had similar Kappa value (0.80 and 0.82, respectively), meaning that the classification is not likely to occur by chance.

Concerning the classification by class type, while all methods were able to successfully classify the soil with a good accuracy, the other vegetation class was the least performant in the RF and ANN. As for the misclassifications, in the SVM classifier, only three samples were wrongly classified in the soil and shadow classes. However, other vegetation and grapevine classes presented wrong classifications in soil and shadow classes, respectively. The RF classifier presents the best overall f1-score in the classification of grapevines and other vegetation, while the ANN presented the best results for soil and shadow classes.

The area predicted in each class per model, in the analysed 0.34 ha vineyard plot is presented in Fig. 3. The prediction from the ANN showed and higher area for soil, shadow and grapevine classes, when compared to the area predicted by the other two classifiers. As for the other vegetation class, the SVM classifier predicted a higher area while the lower area was predicted by the ANN (1280 m^2 and 945 m^2, respectively). Moreover, the SVM showed the lowest estimated area of soil with 1633 m^2.
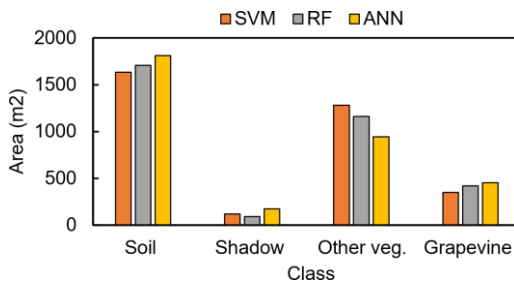

Fig. 3. Area of each class per model from the grapevine classification.

Class	1	2	3	4	F1	OA (%)
Support Vector Machine						
1	229	3	0	0	0.77	
2	3	82	0	0	0.33	45.29
3	89	27	34	5	0.36	
4	39	299	0	40	0.19	
Random Forest						
1	198	0	34	0	0.87	
2	3	63	16	3	0.83	87.76
3	23	1	125	6	0.72	
4	0	2	16	360	0.96	
Artificial Neural Network						
1	214	1	17	0	0.89	
2	1	69	9	6	0.88	86.12
3	33	1	117	4	0.68	
4	1	1	44	332	0.92	

Therefore, through the analysis of the results, it is possible to state that both RF and ANN classifiers, were able to perform vineyard classification with a good performance. However, the prediction stage performed on the whole vineyard, resulted in distinct results. Thus, it is necessary to perform further experiments to study the classification errors. Lastly, the results obtained by the SVM classifier were not satisfactory, providing misclassifications on the grapevine class, being classified as shadow.

The final classified maps can help the farmers/winegrowers into obtaining a general overall context of the vineyard. Fig. 4. shows part of the vineyard classification from the objects generated from OBIA.
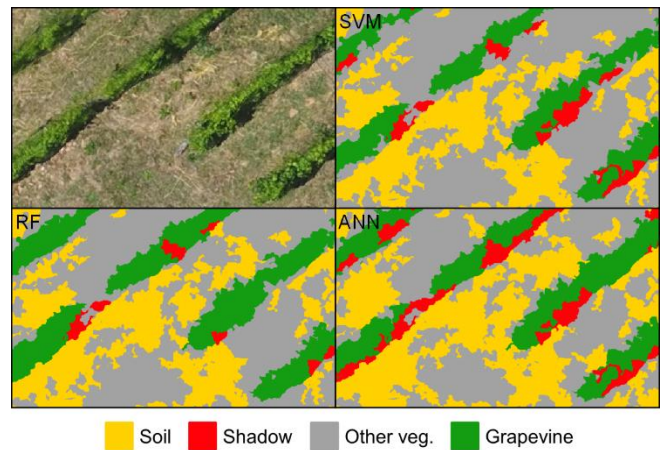

Fig. 4. Part of the classification results of the models in the objects from the object-based image analysis procedure.

6311

4. CONCLUSIONS

In this study UAV-based outcomes from photogrammetric processing were used to evaluate three machine learning approaches for classification purposes. Regarding the four classes defined, the SVM was the least performant method. Contrary to the SVM, the grapevine vegetation detection presented good results in RF and ANN classifiers, which, the RF classifier presented the best performance. However, given the small differences in kappa and overall accuracy between these two methods, more experiments are needed.

Considering that this study only relied in a low-cost RGB sensor, the obtained results are promising. However, the investigation must be performed in other vineyards, with different levels of bare soil and shadow presence, in order to study the behaviour of the classifiers in different contexts. Moreover, the use of UAV-based data from other sensors (thermal infrared and multi-spectral) could be explored to infer the improvements in vineyard classification accuracy. Also comparing unsupervised data clustering approaches and pixel-based approaches should be considered.

ACKNOWLEDGMENTS

5. REFERENCES

[1]   A. Nolan, S. Park, S. Fuentes, D. Ryu, and H. Chung, "Automated detection and segmentation of vine rows using high resolution UAS imagery in a commercial vineyard," presented at the Proceedings of the 21st International Congress on Modelling and Simulation, Gold Coast, Australia, 2015, vol. 29, pp. 1406–1412.

[2]   L. Comba, A. Biglia, D. Ricauda Aimonino, and P. Gay, "Unsupervised detection of vineyards by 3D point-cloud UAV photogrammetry for precision agriculture," *Computers and Electronics in Agriculture*, vol. 155, pp. 84–95, Dec. 2018, doi: 10.1016/j.compag.2018.10.005.

[3]   I. Kalisperakis, C. Stentoumis, L. Grammatikopoulos, and K. Karantzalos, "Leaf area index estimation in vineyards from UAV hyperspectral data, 2D image mosaics and 3D canopy surface models," *The International Archives of Photogrammetry, Remote Sensing and Spatial Information Sciences*, vol. 40, no. 1, p. 299, 2015.

[4]   C. Poblete-Echeverría, G. F. Olmedo, B. Ingram, and M. Bardeen, "Detection and Segmentation of Vine Canopy in Ultra-High Spatial Resolution RGB Imagery Obtained from Unmanned Aerial Vehicle (UAV): A Case Study in a Commercial Vineyard," *Remote Sensing*, vol. 9, no. 3, p. 268, Mar. 2017, doi: 10.3390/rs9030268.

[5]   L. Comba, P. Gay, J. Primicerio, and D. Ricauda Aimonino, "Vineyard detection from unmanned aerial systems images," *Computers and Electronics in Agriculture*, vol. 114, pp. 78–87, Jun. 2015, doi: 10.1016/j.compag.2015.03.011.

[6]   C. J. Tucker, "Red and photographic infrared linear combinations for monitoring vegetation," *Remote Sensing of Environment*, vol. 8, no. 2, pp. 127–150, May 1979, doi: 10.1016/0034-4257(79)90013-0.

[7]   S. Kawashima and M. Nakatani, "An Algorithm for Estimating Chlorophyll Content in Leaves Using a Video Camera," *Ann Bot*, vol. 81, no. 1, pp. 49–54, Jan. 1998, doi: 10.1006/anbo.1997.0544.

[8]   J. Bendig *et al.*, "Combining UAV-based plant height from crop surface models, visible, and near infrared vegetation indices for biomass monitoring in barley," *International Journal of Applied Earth Observation and Geoinformation*, vol. 39, no. Supplement C, pp. 79–87, Jul. 2015, doi: 10.1016/j.jag.2015.02.012.

[9]   D. M. Woebbecke, G. E. Meyer, K. Von Bargen, and D. A. Mortensen, "Color Indices for Weed Identification Under Various Soil, Residue, and Lighting Conditions," *Transactions of the ASAE*, vol. 38, no. 1, p. 259, 1995, doi: 10.13031/2013.27838.

[10]   A. A. Gitelson, Y. J. Kaufman, R. Stark, and D. Rundquist, "Novel algorithms for remote estimation of vegetation fraction," *Remote Sensing of Environment*, vol. 80, no. 1, pp. 76–87, Apr. 2002, doi: 10.1016/S0034-4257(01)00289-9.

[11]   J. Inglada and E. Christophe, "The Orfeo Toolbox remote sensing image processing software," in *2009 IEEE International Geoscience and Remote Sensing Symposium*, Jul. 2009, vol. 4, pp. IV-733-IV–736, doi: 10.1109/IGARSS.2009.5417481.

[12]   J. Michel, D. Youssefi, and M. Grizonnet, "Stable mean-shift algorithm and its application to the segmentation of arbitrarily large remote sensing images," *IEEE Transactions on Geoscience and Remote Sensing*, vol. 53, no. 2, pp. 952–964, 2014.

[13]   C.-C. Chang and C.-J. Lin, "LIBSVM: A library for support vector machines," *ACM Trans. Intell. Syst. Technol.*, vol. 2, no. 3, pp. 1–27, Apr. 2011, doi: 10.1145/1961189.1961199.